RAPID COMMUNICATIONS

PHYSICAL REVIEW E **71**, 060201(R) (2005)

Molecular valves actuated by intermolecular forces

M. A. Snyder and D. G. Vlachos*
Department of Chemical Engineering, University of Delaware, Newark, Delaware 19716-3110, USA

(Received 9 January 2005; published 22 June 2005)

Phase behavior in nanostructured thin films under a gradient in chemical potential is studied via kinetic Monte Carlo simulation. Switching between saturated, partially saturated, and unsaturated states drives precipitous changes in permeation. This phenomenon could render nanostructured thin films as molecular valves, where adsorbate-adsorbate forces actuate the flow of molecules.

DOI: 10.1103/PhysRevE.71.060201 PACS number(s): 61.20.−p, 81.05.Rm, 66.30.Pa, 68.35.Rh

Rationally controlling phase transitions in ordered porous substrates holds unprecedented potential for molecular separations, chemical sensing, and nanoscale materials templating applications. The current drive towards nanotechnology, e.g., [1,2], turns the focus for such applications to crystalline nanostructured materials [e.g., zeolites, metal organic frameworks (MOFs), etc.], having pore sizes approaching molecular dimensions. The small diameter of nanopores, however, cannot support the common capillary condensation [3] mechanism responsible for phase transitions in mesoporous materials. Yet, experimental studies have identified adsorbate phase transitions within such materials under certain conditions [4–8] and suggested [5] that such phase behavior occurs as the adsorbed phase transitions from a fluidlike to a solidlike state. Complementary theoretical studies [9–13] conclude that equilibrium phase transitions within nanostructured materials derive from correlation effects induced by short-range and long-range (i.e., spanning neighboring pores or supercages) adsorbate-adsorbate interactions. The development of thin, nanostructured films with preferred orientation, e.g., [14], has spawned a large body of research into membrane applications. Yet, these membrane studies have typically focused on system conditions far from critical points.

Here, we investigate the behavior of interacting adsorbates in nanostructured thin films under a gradient in chemical potential near system criticality. Confined diffusion of strongly adsorbing molecules in nanostructured systems is often governed by rare-event dynamics. Kinetic Monte Carlo (KMC) is an ideal technique for simulating such systems. Here, we employ a three-dimensional (3D) cubic lattice gas representation of potential energy minima (i.e., binding sites) of the film. The film is terminated at parallel planes (i.e., boundaries) separated by n lattice units of distance a, yielding a film thickness of $L=na$. Periodic boundary conditions are imposed in the directions parallel to the film boundaries, and the film is contacted with two constant but different chemical potential gas reservoirs to perform nonequilibrium KMC calculations. Details of gradient KMC simulations are outlined in [15].

Exchange of molecules between the gas and the film occurs via adsorption to and desorption from the terminal binding sites. These microscopic processes are selected with transition probabilities per unit time of $\Gamma_{ads,i}=k_a P(1-\theta_i)$ and $\Gamma_{des,i}=k_{d,i}\theta_i \exp[-\beta(|\Delta H^o_{a,i}|+\Sigma_{k\in N,k\neq i}J_k\theta_k)]$ for adsorption and desorption, respectively. Here, k_a is the adsorption rate constant, P is the gas pressure, θ_i is the local order parameter of site i (0 or 1 for an empty or occupied site, respectively), k_d is the zero-coverage frequency of desorption, $\beta=(kT)^{-1}$ is the inverse thermal energy, $\Delta H^o_{a,i}$ is the zero-coverage heat of adsorption on site i, J_k is the adsorbate-adsorbate intermolecular potential, and N is the set of binding sites falling within the potential cutoff radius, L_p, of site i. For proof of concept, we consider diffusion along one-dimensional pores via Arrhenius dynamics [15] in the presence of attractive first- and second-nearest-neighbor adsorbate-adsorbate interactions with a transition probability $\Gamma_{i\rightarrow j}=k_{mig,ij}\theta_i\exp[-\beta(U_{o,ij}+\Sigma_{k\in N,k\neq i}J_k\theta_k)]\Sigma_{j=1}^{Z}(1-\theta_j)$. Here, $k_{mig,ij}$ and $U_{o,ij}$ are the zero-coverage frequency and site-to-site activation energy of migration, respectively, and the summation extends over all possible neighboring sites up to the coordination number Z. We employ a 3D, piecewise constant potential, $J_k=\{J_o/N, 1\leqslant|r-r'|\leqslant L_p; 0, |r-r'|>L_p\}$, to describe interactions between molecules at positions r' and r within L_p. Both interpore and intrapore adsorbate-adsorbate forces within the cutoff radius are included.

We employ natural parameter continuation to predict flux and average loading (spatial or spatiotemporal average of θ_i for transient or steady-state simulations, respectively) for thin films of varying thickness. Hereafter, $a=2$ nm is assumed, and films of varying thickness are employed. KMC simulations trace solution branches by initializing the lattice at each new temperature with the final lattice occupancies from the previous temperature. We discard the first 10^6 MC steps (a step is equal to the number of sites) of each KMC simulation, and collect statistics for an additional 10^6 MC steps. Below, we refer to discontinuous changes in loading over a small (~1 K) change in temperature interchangeably as "transition" or "turning point" temperatures.

Analysis reveals interesting behavior depicted in Fig. 1(a). For the thinnest films ($L=8$ and 16 nm), a precipitous increase in flux over several orders of magnitude is observed upon heating the system, concomitant with a similarly precipitous decrease in spatiotemporal average loading depicted in Fig. 1(b). This nearly reversible phenomenon, occurring as the transition temperature, clearly shows that phase transitions within nanostructured materials do persist under gradi-

---

*Corresponding author. Email address: vlachos@che.udel.edu

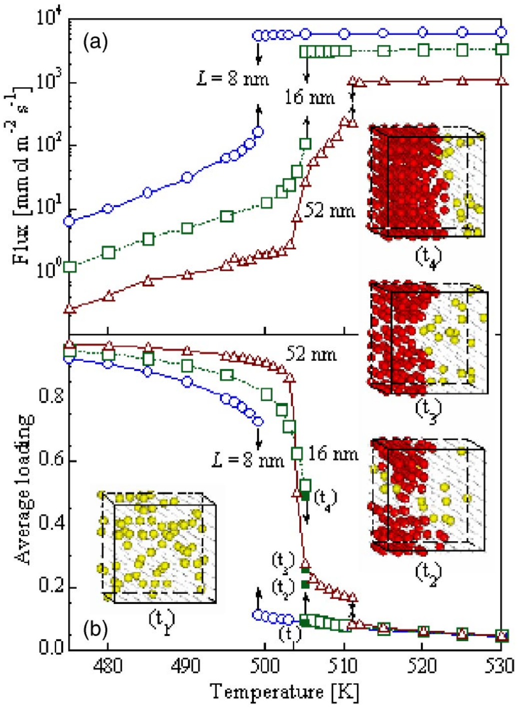

FIG. 1. (Color online) Flux (a) and spatiotemporal average loading (b) in nanostructured films of indicated thickness under a small gradient in chemical potential ($\Delta P = 3.1$ kPa, $P_{\mathrm{high}} = 6.7$ kPa, $\beta J_o = 4$, $\Delta H_a^o = -32.0$ kJ/mol, $k_d = 10^{13}$ s^{-1}, k_a calculated via kinetic theory with unity sticking coefficient, $U_o = 32$ kJ/mol, and $k_{mig,ij} = 5.1 \times 10^{12}$ s^{-1}). Insets show constant temperature snapshots of the $L = 16$ nm film at increasing times depicted as filled squares labeled t_1 through t_4 in panel (b).

ents in chemical potential. However, the apparent annihilation or narrowing of metastable regions in comparison to hysteresis loops observed under equilibrium conditions (analyzed later) reveals behavior characteristic of gradient-driven phase transitions.

The resulting temperature resolution of the transition temperature, just ±1 K, is striking given the small-sized systems modeled. KMC simulations at the transition temperature, shown in Figs. 2(a) and 2(b), reveal temporal fluctuations in the spatial average loading for thinner films. The bimodal nature of the corresponding probability density functions (PDF) depicted in the right-hand portion of Figs. 2(a) and 2(b) clearly shows the two distinct states accessed. This “on/off” of permeation or “opening” and “closing” of flux effectively renders thin nanostructured films as molecular valves capable of actuating molecular flow channels.

Representative snapshots of sufficiently thin films during a transition from an unsaturated state to a saturated state are shown as insets for increasing times t_1 through t_4 in Fig. 1 corresponding to the solid square symbols in Fig. 1(b). Small gray points represent vacant binding sites along the one-dimensional pores passing horizontally from left (in contact with the high-pressure reservoir) to right (in contact with the low-pressure reservoir). Molecules are depicted as large spheres. Mobile molecules are shaded light gray, whereas clusters of molecules are shaded dark gray.

At short times, the film is unsaturated (inset t_1). This state is representative of high-temperature conditions, where interactions are diminished and molecules diffuse readily through the film. With increasing time, strong attractive forces spanning nearest- and next-nearest-neighboring pores facilitate nucleation of 3D molecular clusters (dark molecules in inset t_2) near the high-pressure side of the film. Growth of these clusters, depicted in inset t_3, arises as they trap molecules from the high-pressure reservoir. Finally, phase transition proceeds through rapid propagation of the high-density phase towards the low-pressure side of the film (a behavior that is reminiscent of a traveling wave), effectively closing the majority of diffusion pathways (inset t_4). The result is a sudden, orders-of-magnitude decrease in the flux. In this saturated state, permeation occurs only through rare diffusion of molecules able to escape from the high-density clusters due to the single file diffusion nature [16,17] of permeation. Yet, this behavior also persists in KMC simulations (not shown) of 3D diffusion, emphasizing the generality of the observed phenomenon. Below the transition temperature, the film is almost fully saturated (no corresponding snapshot).

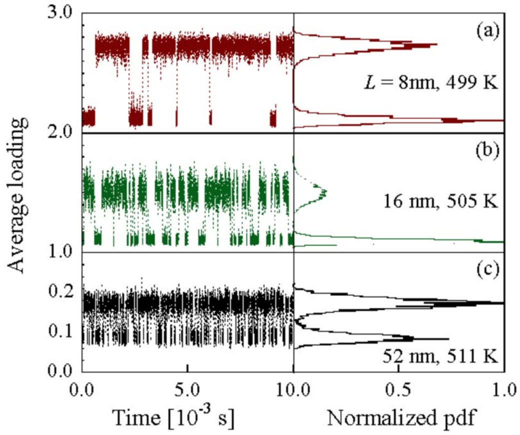

FIG. 2. (Color online) Spatial average loading trajectories (left panel) shifted vertically for clarity at constant temperatures. Normalized PDFs are shown to the right.

For thicker ($L = 52$ nm) films, a phase behavior is observed with changing temperature where two distinct transitions occur between three different film saturation states. The low-temperature transition is marked by a substantial decrease in loading from a saturated to a partially saturated state and more than an order-of-magnitude increase in flux with a small change (~2 K) in temperature (“off” to “partially on” operation). A gradual change in properties occurs upon further increase of temperature up to the high-temperature transition (“partially on” to “on” operation). The high-temperature transition exhibits the features of thinner membranes between two distinct partially saturated and unsaturated states, as shown in Fig. 2(c), and a concomitant order-of-magnitude change in flux.

The low-temperature transition in thicker membranes exhibits interesting dynamics. Figure 3 shows three steady-state coverage profiles depicting saturated (solid symbols), unsaturated (open symbols), and partially saturated (profiles with no symbols) thin film states. The first two are characteristic of thinner membranes discussed above, whereas the partially saturated one is a state found in thicker membranes

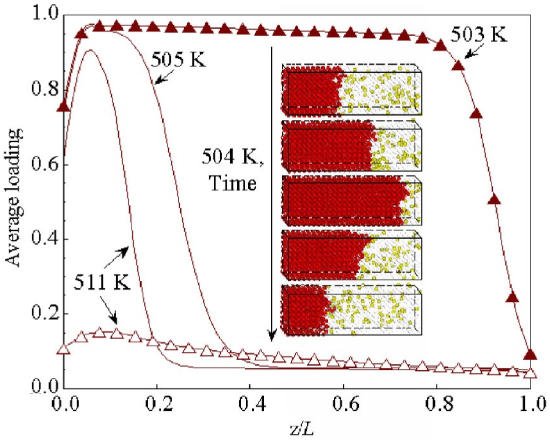

FIG. 3. (Color online) Steady-state axial loading profiles for the $L=52$-nm-thick film at various temperatures. Insets depict snapshots during about half the period of oscillations.

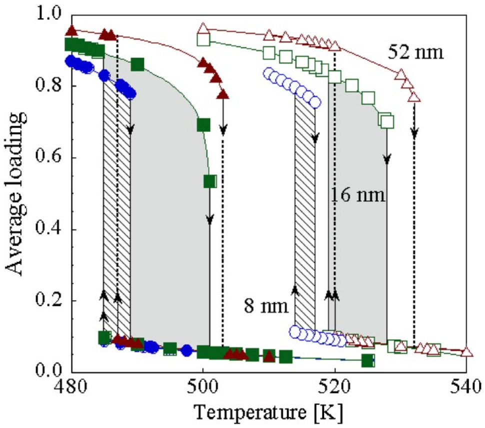

FIG. 4. (Color online) Comparison of equilibrium loadings in films of finite thickness, L, indicated for pressures corresponding to the low- (filled symbols) and high- (open symbols) pressure reservoirs of the simulations in Fig. 1.

only. The snapshots, shown in Fig. 3, depict oscillations during roughly half a period at the low-temperature transition of a traveling-wave-like filling and partial emptying of the membrane.

Insight into the finite-size effects shown in Figs. 1–3 is obtained by studying the temperature dependence of local equilibrium (LE) at the boundaries, following the criterion proposed in [18]. Qualitatively, LE is achieved when adsorption and desorption rates are fast compared to diffusion within the film. LE at both boundaries implies that the two boundaries are practically decoupled. For thinner films (e.g., $L=8$ and 16 nm), LE persists only at the high-pressure boundary as temperature increases from low values. At the transition temperature, deviations from LE even at the high-pressure boundary result in a collective transition of the entire film to the unsaturated state. The dual transition observed in thicker films ($L=52$ nm) could be likewise explained. At the low-temperature transition, LE holds at both boundaries implying decoupling of the boundaries in thicker systems. Thus, the first transition affects only the low-pressure side of the film. The partial emptying renders the effective, saturated thickness of a thicker membrane comparable to that of thin membranes at their single transition (compare Figs. 1 and 3). Consequently, the behavior (e.g., LE and dynamics) at the high-temperature transition is similar to that of thinner membranes.

Equilibrium phase envelopes are shown in Fig. 4 for finite thickness films in contact with gas reservoirs of identical chemical potential at both sides. Here, the pressures are equivalent to the high (open symbols) and low pressures (closed symbols) of the system considered previously. Similar to the gradient systems, finite-size effects are manifested in the shrinking and shifting of the phase envelopes to lower temperatures for thinner systems. The existence of hysteresis loops under equilibrium conditions (Fig. 4), however, is in striking contrast to the apparent narrowing or absence of metastability observed for the forced systems studied above (Fig. 1).

Here we have a simple potential, yet the molecular valve phenomenon should persist with more complex interactions. Sensitivity analysis (not shown) of the transition temperatures with respect to the interaction strength showed that the transition temperature is reduced with decreasing interaction strength with a relatively high sensitivity ranging from 5 to 45 $\mathrm{K/(kcal\,mol^{-1})}$. At large interaction strengths, slightly irreversible valves develop, with stronger actuation leading to even more dramatic changes in the flux.

Harnessing the sensitivity of this phenomenon requires an understanding of viable transition temperatures and design of compatibility between target molecules and materials. In a forthcoming communication [19], we employ a hierarchical mesoscopic approach to explore how changes in host-guest properties can lead to different transition temperatures. This is further evidenced in the work of [10–12], who studied equilibrium systems defined by weak and strong adsorbate-substrate interactions and observed an order-of-magnitude difference in critical temperatures. From a materials perspective, experimental evidence [4,5] has shown that phase transitions are facilitated by agreement between adsorbate molecular dimensions and binding site spacing. The host of available nanostructured materials offers a means to accomplish this task. As an example, cation content in zeolites could conceivably be employed to tune binding sites for control of lattice dimension compatibility and heats of adsorption, evidenced by experiments [5,7] showing the dependency of equilibrium phase transitions upon cation content. MOFs [20], shown recently to yield equilibrium hysteresis loops of interest for hydrogen storage applications [2], offer another possibility. In addition, a novel "gate" phenomenon identified for the titanosilicalite ETS [21] is an interesting case in which a structural phase transition occurs with changing temperature. The gate transition, which is mathematically congruous with the molecular valve phenomenon observed here for the adsorbed phase, presents an additional means for tuning substrate properties. Moreover, the combination of the "gate" and "valve" phenomena has potential applications for "smart" host-guest systems.

Conceivable application of the molecular valve phenomenon includes sensing of target molecules with nanostructured films, rationally designed (e.g., tuning of film thickness and system temperature) based upon molecule-material compatibility. Furthermore, the persistence of this phenomenon at the low pressures studied here is encouraging evidence of its viability for low-concentration sensing. The "opened"-"closed" mechanism could also be employed as a temperature actuated diffusion barrier for applications reminiscent of hydrocarbon trapping presented in [22]. In particular, a nanostructured material in a saturated state could be designed for temperature-sensitive release or containment of a second adsorbing/diffusing species. Such applications would require the as yet unexplored understanding of the effect of multicomponent diffusion upon the molecular valve phenomenon.

In summary, we have illustrated the persistence of phase transitions in thin nanostructured films under chemical potential gradients with conceivable generality to systems driven by other external fields (e.g., magnetic and electric). We have identified a behavior whereby metastability is reduced or annihilated under forced conditions for thin films. The abrupt phase change of adsorbates diffusing in nanostructured thin films is accompanied by precipitous changes in flux giving rise to an "on/off" permeation behavior reminiscent of mechanical valves. Finite-size effects shift phase behavior, and give rise, in thicker nanostructured films, to an additional phase transition between saturated and partially saturated states with traveling-wave-like oscillations between them associated with partial emptying and filling of the film.

This research was partially supported by NSF through Grants No. ITR-0219211 and No. CTS-0343757.

[1] C. Bichara, J. Y. Raty, and R. J.-M. Pellenq, Phys. Rev. Lett. **89**, 016101 (2002).
[2] X. Zhao *et al.*, Science **306**, 1012 (2004).
[3] K. Binder and D. P. Landau, J. Chem. Phys. **96**, 1444 (1992).
[4] C. Martin *et al.*, Langmuir **14**, 1774 (1998).
[5] P. L. Llewellyn *et al.*, Langmuir **9**, 1846 (1993).
[6] O. Talu, C.-J. Guo, and D. T. Hayhurst, J. Phys. Chem. **93**, 7294 (1989).
[7] D. H. Olsen, G. T. Kokotailo, and S. L. Lawton, J. Phys. Chem. **85**, 2238 (1981).
[8] R. E. Richards and L. V. C. Rees, Zeolites **8**, 35 (1988).
[9] I. Leike and F. Marlow, Zeolites **16**, 65 (1996).
[10] R. Radhakrishnan and K. E. Gubbins, Phys. Rev. Lett. **79**, 2847 (1997).
[11] C. Saravanan and S. M. Auerbach, J. Chem. Phys. **109**, 8755 (1998).
[12] I. Dukovski *et al.*, J. Chem. Phys. **113**, 3697 (2000).
[13] D. Douguet *et al.*, Mol. Simul. **17**, 255 (1996).
[14] Z. Lai *et al.*, Science **300**, 456 (2003).
[15] D. G. Vlachos and M. A. Katsoulakis, Phys. Rev. Lett. **85**, 3898 (2000).
[16] K. Hahn, J. Karger, and V. Kukla, Phys. Rev. Lett. **76**, 2762 (1996).
[17] D. S. Sholl and K. A. Fichthorn, J. Chem. Phys. **107**, 4384 (1997).
[18] S. Kalamatianos, Y. K. Park, and D. G. Vlachos, Combust. Flame **112**, 45 (1998).
[19] M. A. Snyder and D. G. Vlachos, J. Chem. Phys. (to be published).
[20] R. Q. Snurr, J. T. Hupp, and S. T. Nguyen, AIChE J. **50**, 1090 (2004).
[21] S. M. Kuznicki *et al.*, Nature (London) **412**, 720 (2001).
[22] K. F. Czaplewski *et al.*, Microporous Mesoporous Mater. **56**, 55 (2002).